

Charge and Spin Ordering in Monoclinic Nb<sub>12</sub>O<sub>29</sub>

J. E. L. Waldron, M. A. Green,\* and D. A. Neumann†

Royal Institution of Great Britain  
21 Albemarle Street, London, W1X 4BS U.K.  
NIST Center for Neutron Research  
National Institute of Standards and Technology  
Gaithersburg, Maryland 20899

Received January 4, 2001  
Revised Manuscript Received April 30, 2001

There are a number of properties unique to one-dimensional systems,<sup>1</sup> such as the spin-Peierls transition, which makes them of great interest. One-dimensional properties are usually inherent in the structure, that is, they are composed of electronically active chains separated by inert ligands. The distance between these chains determines the degree of low dimensionality. For this reason, materials containing bulky organic ligands often give the most desirable properties, as there are sufficiently large distances between chains for true low-dimensional character to occur. Here we show how the phenomenon of charge ordering, where different oxidation states are localized onto crystallographically distinct sites, creates comparable properties in a condensed inorganic oxide phase. Charge ordering, has played an increasingly important role in solid-state sciences over the past few years. This has been exemplified recently in the complex relationship between spin, charge, and orbital ordering in perovskite manganates displaying colossal magnetoresistance.<sup>2</sup> Although it is a relatively subtle phenomenon and often difficult to detect directly with structural measurements, it can have a profound influence on the physical properties of a material. The ordering of ions with different oxidation states within a structure can be caused by a variety of electronic or structural factors. A common driving force is the desire for two different oxidation states in the same coordination to adopt different geometries. For example, the out-of-center distortion in octahedra containing d<sup>0</sup> ions causes NaV<sub>2</sub>O<sub>5</sub> to form chains of V<sup>4+</sup> (d<sup>1</sup>) and V<sup>5+</sup> (d<sup>0</sup>) ions at low temperature.<sup>3</sup> Although these properties have been apparent for a number of years, there has been relatively little work in the actual manipulation of this phenomenon to develop materials with unique physical properties.

Orthorhombic Nb<sub>12</sub>O<sub>29</sub> was reported as the first example of a magnetically ordered system containing 4d<sup>1</sup> or 4d<sup>2</sup> electrons, which is unusual due to their preference for itinerant behavior through strong metal–metal overlap. It was shown to be metallic with an antiferromagnetic transition at 12 K.<sup>4,5</sup> No physical property measurements have been carried out on monoclinic Nb<sub>12</sub>O<sub>29</sub> due to the difficulty in preparing a pure bulk phase sample. Compounds in this work were prepared by first forming H–Nb<sub>2</sub>O<sub>5</sub> by heating as supplied Nb<sub>2</sub>O<sub>5</sub> to 1100 °C for 24 h. H–Nb<sub>2</sub>O<sub>5</sub> was reduced using Nb metal in a sealed evacuated quartz tube for 1 h at 1200 °C, followed by rapid quenching to room temperature. Susceptibility and conductivity measurements of monoclinic Nb<sub>12</sub>O<sub>29</sub>, performed on a Quantum Design MPMS7 SQUID magnetometer and Oxford Instruments Maglab<sup>2000</sup> system, respectively, revealed identical properties to its orthorhombic analogue, with a transition at 12 K to an antiferromagnetic state despite its metallic character over the 2–300 K temperature range. This is a surprising result if we consider the concentration of unpaired electrons. Monoclinic Nb<sub>12</sub>O<sub>29</sub> has a crystallographic

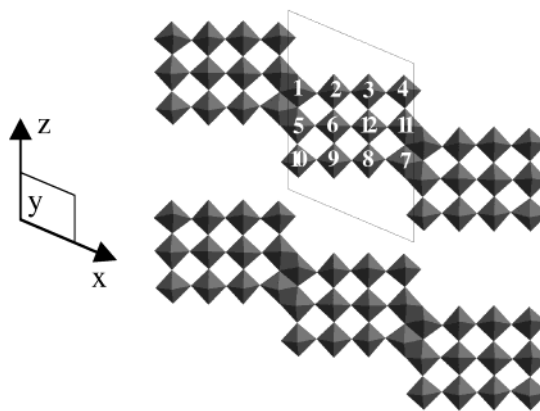


**Figure 1.** The crystallographic shear plane structure of monoclinic Nb<sub>12</sub>O<sub>29</sub> composed of 4 × 3 blocks of corner-shared NbO<sub>6</sub> units which are edge-shared to their adjacent block as obtained from Rietveld refinement at room temperature in the *A2/m* space group.

shear plane structure composed of 4 × 3 blocks of NbO<sub>6</sub> octahedra, which are edge-shared to the next block in a diagonal arrangement as shown in Figure 1. The formula can be rewritten as Nb<sup>4+</sup><sub>2</sub>Nb<sup>5+</sup><sub>10</sub>O<sub>29</sub>. Nb<sup>5+</sup> has the electronic configuration of d<sup>0</sup> and is diamagnetic, whereas Nb<sup>4+</sup> is d<sup>1</sup> (*S* = 1/2); therefore, there are two unpaired electrons per block. The Curie constant obtained from fitting the susceptibility data to the Curie–Weiss law at high temperature (*C* = 0.321 emu K mol<sup>−1</sup> and *θ* = −26.36 K) shows 48% of these electrons are contributing to the localized nature of the material, the rest being itinerant, as reported for orthorhombic Nb<sub>12</sub>O<sub>29</sub>.<sup>4</sup> For a system containing 1 localized spin in 12, embedded in a sea of conduction electrons, the most likely result is the formation of a spin glass state; that is, the spins are frozen at low temperature in a disordered arrangement, seen in many systems such as mixed metal alloys.<sup>6</sup> Antiferromagnetic ordering is a long-range phenomenon; therefore, the spins need to be arranged in a particular well-defined arrangement throughout the entire lattice. The long-range nature of magnetic ordering in monoclinic Nb<sub>12</sub>O<sub>29</sub>, rather than a spin glass state, is confirmed by the overlap of the zero field cooled and field cooled susceptibility and discrete oscillations in a zero field cooled μSR experiment.<sup>7</sup>

To investigate how the magnetic ordering occurs a series of neutron diffraction experiments were performed on the BT1 diffractometer at the National Institute of Standards and Technology, MD, U.S.A. (*λ* = 1.5401 Å at 300 K and *λ* = 2.078 Å, at 25 K and 4 K) and the D2b diffractometer at the Institute Laue Langevin, Grenoble, France (*λ* = 1.594 Å and *λ* = 2.398 Å at 2 K and *λ* = 1.594 Å at 30 K). The structure of monoclinic Nb<sub>12</sub>O<sub>29</sub> at room temperature was refined in the *A2/m* space group and is therefore isostructural with Ti<sub>2</sub>Nb<sub>10</sub>O<sub>29</sub><sup>8</sup> as opposed to the *A2/a* space group proposed by Norin.<sup>9</sup> On cooling the sample, the thermal parameters, which were constrained to be identical for all Nb and all O atoms to reduce the number of parameters in the refinement, decreases as expected (300 K, Nb = 0.0129(28) Å<sup>2</sup>, O = 0.011(23) Å<sup>2</sup>, 25 K Nb = 0.0100(25) Å<sup>2</sup>, O = 0.0053-(19) Å<sup>2</sup>) until 4 K, where there is a significant increase (Nb = 0.0121(14) Å<sup>2</sup>, O = 0.0086(13) Å<sup>2</sup>), which is often an indication of a structural phase transition. This was further supported by the quality of the Rietveld fit, which had unaccounted scattering in a number of regions. However, there were no additional

† NIST.

(1) Katsumata, K. *Curr. Opin. Solid State Mater. Sci.* **1997**, 2, 226.  
(2) Rao, C. N. R.; Arulraj, A.; Cheetham, A. K.; Raveau, B. *J. Phys.: Condens. Matter* **2000**, 12, R83.  
(3) Hase, M.; Terasaki, I.; Uchinokura, K. *Phys. Rev. Lett.* **1993**, 23, 3651.  
(4) Cava, R. J.; Batlogg, B.; Krajewski, J. J.; Gammel, P.; Poulson, H. F.; Peck, W. F.; Rupp, L. W. *Nature* **1991**, 350, 598.  
(5) Cava, R. J.; Batlogg, B.; Krajewski, J. J.; Poulson, H. F.; Gammel, P.; Peck, W. F.; Rupp, L. W. *Phys. Rev. B* **1991**, 44, 6973.

(6) Mydosh, J. A. *Spin Glasses: An Experimental Introduction*; Taylor and Francis: London, 1993.

(7) Waldron, J. E. L. Thesis, University of London, 2000.

(8) Wadsley, A. D. *Acta Crystallogr.* **1961**, 14, 664.

(9) Norin, R. *Acta Chem. Scand.* **1966**, 20, 871.

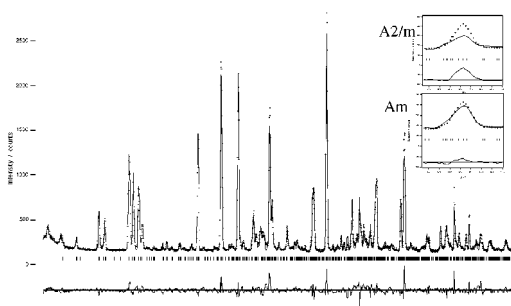


**Figure 2.** Rietveld refinement of monoclinic  $\text{Nb}_{12}\text{O}_{29}$  at 2 K and  $\lambda = 1.594 \text{ \AA}$ . The inset shows an expansion of a region around  $60^\circ$  for the refinements in both the  $A2/m$  and  $Am$  space groups, as an example of the significant improvement gained with the use of the lower symmetry configuration.

reflections, suggesting the systematic absences associated with the A-centered space group were incorrect. Therefore, the lattice symmetry was reduced to  $Am$  which caused a considerably improved fit to the observed data. This is verified by a significant improvement in the goodness-of-fit factors ( $A2/m \lambda = 1.594 \text{ \AA}$ ,  $R_{\text{wp}} = 9.69\%$ ,  $\lambda = 2.398 \text{ \AA}$ ,  $R_{\text{wp}} = 12.29\%$  to  $Am \lambda = 1.594 \text{ \AA}$ ,  $R_{\text{wp}} = 8.77\%$ ,  $\lambda = 2.398 \text{ \AA}$ ,  $R_{\text{wp}} = 11.91\%$ ). No magnetic scattering was observed due to the incommensurate<sup>7</sup> and dilute nature of the magnetic structure. A representative diagram of the quality of the fit is shown in Figure 2, which also shows an inset of the region around  $60^\circ 2\theta$ , confirming the greatly improved fit in the  $Am$  space group.

The Rietveld refinements of the 25 or 30 K datasets were not improved upon by use of the  $Am$  space group, implying the phase transition occurs between 25 and 2 K, which corresponds to the temperature range in which the antiferromagnetic ordering also occurs. In the  $A2/m$  space group, the 2-fold rotation constrains six of the Nb positions to adopt identical geometry to the other six. The main structural difference with the  $Am$  space group, is that all 12 Nb positions are crystallographically inequivalent; in other words, each  $\text{NbO}_6$  octahedra can adopt different geometries. A close inspection of the Nb–O bond distances reveals the driving force behind the phase transition. Transition metal ions in an octahedral environment have greatly differing geometries for  $d^0$  and  $d^1$  electronic configurations. This is due to an out-of-center distortion in  $d^0$  systems of which  $\text{BaTiO}_3$  is a typical example. This leads to four roughly equal bonds and one which is considerably shorter and one which is considerably longer. Typical lengths that are reported for  $\text{Nb}_2\text{O}_5$  are 1.983, 1.949, 2.001, 1.983, 1.800, and 2.270  $\text{\AA}$ .<sup>10</sup> In contrast, transition metal oxides containing  $d^1$  electronic configurations do not undergo this distortion and have all six bond distances in their octahedra roughly equivalent. We can mathematically define this by calculating a bond length variance factor,  $s$ , which is an indication of the degree the  $n$  bonds of length,  $r$ , vary from the mean value,  $r_0$  and defined as

$$s = \frac{1}{n} \sum_n |r - r_0|$$

Octahedra containing  $d^1$  ions will give small values of  $s$ , whereas  $d^0$  octahedra will give larger values. The average bond length and bond length variance for monoclinic  $\text{Nb}_{12}\text{O}_{29}$  at 2 K in the  $Am$  space group are given in Table 1 and show position 12 (defined in Figure 1) to possess a variance over 5 times smaller than any of the other sites. The bond distances for this octahedra are 1.982(30), 1.920(32), 1.99(4), 1.976(8), 1.976(8), and 1.97(4)  $\text{\AA}$ . Refinement in the same space group of the D2b data performed at 30 K shows large variance, and, more importantly, one short and one long bond for all positions. In particular, site

**Table 1.** Average Bond Length and Bond Length Variance for Each Nb Position (the Numbers Refer to Those in Figure 1) Showing All the Bond Lengths Are Very Similar for the Corner-Shared Position (12), in Contrast to the Other 11 Indicating Ordering of the  $\text{Nb}^{4+}$  Ions

Nb site	average bond length ( $\text{\AA}$ )	bond length variance ( $\text{\AA}$ ) 30 K	bond length variance ( $\text{\AA}$ ) 2 K
1	2.031	0.0983	0.3043
2	1.995	0.1213	0.1398
3	2.020	0.0847	0.1103
4	2.042	0.1100	0.0855
5	2.078	0.0600	0.0910
6	1.906	0.1010	0.0903
7	2.082	0.2837	0.2030
8	2.110	0.2490	0.3427
9	2.119	0.2437	0.1520
10	2.016	0.1850	0.1367
11	2.043	0.1570	0.2263
12	1.969	0.1973	0.0163

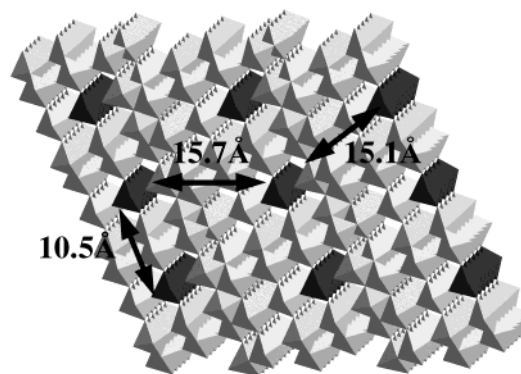


**Figure 3.** Structure of monoclinic  $\text{Nb}_{12}\text{O}_{29}$  showing the ordering of the  $\text{Nb}^{4+}$  ions onto a specific corner-shared positions creating a chain of electronically active ions surrounded by diamagnetic  $\text{Nb}^{5+}$  sites. The chains are the cause of an antiferromagnetic transition in the magnetic susceptibility at 12 K.

12 at 30 K has bond distances of 2.58(8), 1.58(7), 1.98(8), 1.924(7), 1.924, and 1.94(8)  $\text{\AA}$ , proving that the structure is  $A2/m$  at 30 K. This is firm evidence that the site contains a  $\text{Nb}^{4+}$  ( $d^1$ ) ion and that the phase transition is due to the localization of half of the unpaired electrons onto this crystallographically distinct site.

Figure 3 shows the structure of monoclinic  $\text{Nb}_{12}\text{O}_{29}$  with the  $\text{Nb}^{5+}$  and  $\text{Nb}^{4+}$  sites shaded differently. From this diagram, we can see that the  $\text{Nb}^{4+}$  octahedra are corner-shared with another and thus form chains along the  $b$  axis. This explains how we can generate a long-range ordered state from such a magnetically dilute system. This diagram can also explain why this occurs; all  $\text{NbO}_6$  octahedra around the sides of the  $4 \times 3$  block are edge-shared to another octahedra in some way. An edge-sharing arrangement will give much shorter Nb–Nb distances and therefore direct metal–metal overlap which causes metallic properties. An arrangement containing only corner-shared octahedra will have significantly less overlap and tend to localized behavior. The coexistence of itinerant and localized electrons is therefore a direct consequence of a mixture of corner- and edge-sharing within the structure. We have shown how ordering of  $d^0$  and  $d^1$  ions in monoclinic  $\text{Nb}_{12}\text{O}_{29}$  onto crystallographically distinct sites produces a new one-dimensional magnetic state. This ordering is grossly different from any previously reported for a condensed oxide phase as the chains of spins are much further apart; each chain has six nearest neighbors at distances of  $2 \times 10.5 \text{ \AA}$ ,  $2 \times 15.7 \text{ \AA}$ , and  $2 \times 15.1 \text{ \AA}$  apart.

**Acknowledgment.** We acknowledge the financial support of the EPSRC and provision of beam time by the National Institute of Standards and Technology, MD, and the Institute Laue Langevin, Grenoble.

**Supporting Information Available:** Additional details (PDF). This material is available free of charge via the Internet at <http://pubs.acs.org>.